Continental-scale temperature variability during the last two millennia

PAGES 2k Consortium

Moinuddin Ahmed[1], Kevin J. Anchukaitis[2,3], Asfawossen Asrat[4], Hemant P. Borgaonkar[5], Martina Braida[6], Brendan M. Buckley[2], Ulf Büntgen[7], Brian M. Chase[8,9], Duncan A. Christie[10,11], Edward R. Cook[2], Mark A. J. Curran[12,13], Henry F. Diaz[14], Jan Esper[15], Ze-Xin Fan[16], Narayan P. Gaire[17], Quansheng Ge[18], Joëlle Gergis[19], J Fidel González-Rouco[20], Hugues Goosse[21], Stefan W. Grab[22], Nicholas Graham[23], Rochelle Graham[23], Martin Grosjean[24], Sami T. Hanhijärvi[25], Darrell S. Kaufman[26,*], Thorsten Kiefer[27], Katsuhiko Kimura[28], Atte A. Korhola[25], Paul J. Krusic[29], Antonio Lara[10,11], Anne-Marie Lézine[30], Fredrik C. Ljungqvist[31], Andrew M. Lorrey[32], Jürg Luterbacher[33], Valérie Masson-Delmotte[34], Danny McCarroll[35], Joseph R. McConnell[36], Nicholas P. McKay[26], Mariano S. Morales[37], Andrew D. Moy[12,13], Robert Mulvaney[38], Ignacio A. Mundo[37], Takeshi Nakatsuka[39], David J. Nash[22,40], Raphael Neukom[7], Sharon E. Nicholson[41], Hans Oerter[42], Jonathan G. Palmer[43], Steven J. Phipps[44,45], Maria R. Prieto[35], Andres Rivera[46], Masaki Sano[39], Mirko Severi[47], Timothy M. Shanahan[48], Xuemei Shao[18], Feng Shi[49], Michael Sigl[36], Jason E. Smerdon[2], Olga N. Solomina[50], Eric J. Steig[51], Barbara Stenni[6], Meloth Thamban[52], Valerie Trouet[53], Chris S.M. Turney[44], Mohammed Umer[4,¥], Tas van Ommen[12,13], Dirk Verschuren[54], Andre E. Viau[55], Ricardo Villalba[37], Bo M. Vinther[56], Lucien von Gunten[27], Sebastian Wagner[57], Eugene R. Wahl[58], Heinz Wanner[24], Johannes P. Werner[33], James W.C. White[59], Koh Yasue[60], Eduardo Zorita[57]

[1]Department of Botany, Federal Urdu University of Arts, Science and Technology, Karachi, 75300, Pakistan, [2]Lamont Doherty Earth Observatory, Columbia University, Palisades, NY 10964, USA, [3]Woods Hole Oceanographic Institution, Woods Hole, MA 2543, USA, [4]School of Earth Sciences, Addis Ababa University, Addis Ababa, Ethiopia, [5]Indian Institute of Tropical Meteorology, Pune, 411008, India, [6] Dipartimento di Matematica e Geoscienze, University of Trieste, 34128, Italy, [7]Swiss Federal Research Institute WSL, Birmensdorf, 8903, Switzerland, [8]Département Paléoenvironnements et Paléoclimats (PAL), Université Montpellier, Montpellier, 34095, France, [9]Department of Archaeology, History, Cultural Studies and Religion, University of Bergen, Bergen, 5020, Norway, [10]Laboratorio de Dendrocronología y Cambio Global, Universidad Austral de Chile, Valdivia, 5090000, Chile, [11]Center for Climate and Resilience Research, Universidad de Chile, Santiago, 2777, Chile, [12]Australian Antarctic Division, Kingston, Tasmania 7050, Australia, [13]Antarctic Climate & Ecosystems Cooperative Research Centre, University of Tasmania, Sandy Bay, Tasmania 7005, Australia, [14]Cooperative Institute for Research in Environmental Sciences, National Oceanic and Atmospheric Administration, Boulder, CO 80305, USA, [15]Department of Geography, Johannes Gutenberg University, Mainz, 55099, Germany, [16]Xishuangbanna Tropical Botanical Garden, Chinese Academy of Sciences, Yunnan, 666303, China, [17]Faculty of Science, Nepal Academy of Science and Technology, Lalitpur, Nepal, [18]Institute of Geographical Sciences and Natural Resources Research, Chinese Academy of Sciences, Beijing, 100101, China, [19]School of Earth Sciences, University of Melbourne, Melbourne, VIC 3010, Australia, [20]Departamento Astrofísica y CC de la Atmósfera, Universidad Complutense de Madrid, Madrid, 28040, Spain, [21]Lemaitre Center for Earth and Climate Research, Earth and Life Institute, Université catholique de Louvain, Louvain-la-Neuve, 1348, Belgium, [22]School of Geography, Archaeology and Environmental Studies, University of the Witwatersrand, Wits, 2050, South Africa, [23]Hydrologic Research Center, San Diego, CA 92130, USA, [24]Oeschger Centre for Climate Change Research & Institute of Geography, University of Bern, Bern, 3012, Switzerland, [25]Department of Environmental Sciences, University of

Helsinki, Helsinki, 00014, Finland, [26]School of Earth Sciences and Environmental Sustainability, Northern Arizona University, Flagstaff, AZ 86011, USA, [27]International Project Office, Past Global Changes (PAGES), Bern, 3012, Switzerland, [28]Department of Symbiotic System Science, Fukushima University, Fukushima, 960-1248, Japan, [29]Department of Physical Geography and Quaternary Geology, Stockholm University, Stockholm, 106 91, Sweden, [30]Laboratoire d'Océanographie et du Climat: Expérimentations et Approches Numériques (LOCEAN), Université Pierre et Marie Curie, Paris cedex, 575252, France, [31]Department of History, Stockholm University, Stockholm, 106 91, Sweden, [32]National Institute of Water and Atmospheric Research, Ltd., National Climate Centre Auckland, 1011, Zealand, [33]Department of Geography, Climatology, Climate Dynamics and Climate Change, Justus Liebig University, Giessen, 35390, Germany, [34]Laboratoire des Science du Climat et de l'Environnement, Gif-sur-Yvette, 91 191, France, [35]Department of Geography, Swansea University, Swansea, SA28PP, UK, [36]Desert Research Institute, Nevada System of Higher Education, Reno, NV 89512, USA, [37]Instituto Argentino de Nivología, Glaciología y Ciencias Ambientales (IANIGLA), CCT-CONICET-Mendoza, Mendoza, 5500, Argentina, [38]British Antarctic Survey, Cambridge, CB3 0ET, UK, [39]Department of Earth and Environmental Sciences, Nagoya University, Nagoya, 464.8601, Japan, [40]School of Environment and Technology, University of Brighton, Brighton, BN2 4GJ, UK, [41]Department of Earth, Ocean and Atmospheric Sciences, Florida State University, Tallahassee, FL 32308, USA, [42]Department of Glaciology, Alfred Wegener Institute for Polar and Marine Research in the Helmholtz Association, Bremerhaven, 27570, Germany, [43]College of Life and Environmental Sciences, University of Exeter, Exeter, EX4 4RJ, UK, [44]Climate Change Research Centre, University of New South Wales, Sydney, NSW 2052, Australia, [45]ARC Centre of Excellence for Climate System Science, University of New South Wales, Sydney, Australia, [46]Centro de Estudios Cientificos, Valdivia, Chile, [47]Department of Chemistry "Ugo Schiff", University of Florence, Sesto Fiorentino, 50019, Italy, [48]Jackson School of Geosciences, University of Texas at Austin, Austin, TX 78712, USA, [49]State Key Laboratory of Numerical Modelling for Atmospheric Sciences and Geophysical Fluid Dynamics, Chinese Academy of Sciences, Beijing, 100029, China, [50]Institute of Geography, Russian Academy of Sciences, Moscow, 119017, Russia, [51]Department of Earth and Space Sciences, University of Washington, Seattle, WA 98195, USA, [52]National Centre for Antarctic and Ocean Research, Goa, 403 804, India, [53]Laboratory of Tree-Ring Research, University of Arizona, Tucson, AZ 85721, USA, [54]Department of Biology, Ghent University, Ghent, 9000, Belgium, [55]Department of Geography, University of Ottawa, Ottawa, K1N 6N5, Canada, [56]Niels Bohr Institute, University of Copenhagen, Copenhagen, 2100, Denmark, [57]Institute for Coastal Research, Helmholtz-Zentrum Geesthacht, Geesthacht, 21502, Germany, [58]National Climatic Data Center, National Oceanic and Atmospheric Administration, Boulder, CO 80305, USA, [59]Institute of Arctic and Alpine Research, University of Colorado, Boulder, CO 80309, USA, [60]Department of Forest Science, Shinshu University, Nagano, 399-4598, Japan

*e-mail: Darrell.Kaufman@nau.edu
[¥]Deceased

Past global climate changes had strong regional expression. To elucidate their spatial-temporal pattern, we reconstructed past temperatures for seven continental-scale regions during the last one to two millennia. The most coherent feature in nearly all of the regional temperature reconstructions is a long-term cooling trend, which ended late in the 19th century. At multi-decadal to centennial scales, temperature variability shows distinctly different regional patterns, with more similarity within each hemisphere than between them. There were no globally synchronous multi-decadal warm or cold intervals that define a worldwide Medieval Warm Period or Little Ice Age, but all reconstructions show generally cold conditions between 1580 and 1880 CE, punctuated in some regions by warm decades during the 18th century. The transition to these colder conditions occurred earlier in the Arctic, Europe and Asia than in North America or the Southern Hemisphere regions. Recent warming reversed the long-term cooling; during the last 30-year period (1971-2000 CE), the area-weighted average reconstructed temperature was likely higher than anytime in nearly 1400 years.

During the current interglacial period, Earth's climate has undergone significant climate variations that have yet to be quantified at the continental scale, where climate variability is arguably more relevant to ecosystems and societies than globally averaged conditions. Determining the magnitude of these changes is needed to distinguish anthropogenic impacts from the background range of natural variability[1]. Reconstructing spatiotemporal patterns of past climate variability helps to understand and quantify the influence of externally forced and intrinsic dynamics of the global climate system[2], and to understand natural climate variability, which needs to be considered in future climate scenarios[3,4]. Here we present a global dataset of proxy records and associated temperature reconstructions for seven continental-scale regions. We describe the most prominent features of continental-scale temperature changes

at multi-decadal to millennial time scales. In contrast to other recent global-scale reconstructions[5,6], this study provides an inter-continental perspective of temperature evolution during the Common Era.

PAGES 2k Network and temperature reconstructions

The '2k Network' of the IGBP Past Global Changes (PAGES) project aims to produce a global array of regional climate reconstructions for the last 2000 years (www.pages-igbp.org/science/foci/focus-2/themes/2k-network). Nine PAGES 2k working groups represent eight continental-scale regions (Fig. 1) and the oceans. Regional representation brings critical expert knowledge of individual proxy datasets, which is essential for improving paleoclimate reconstructions[7]. The PAGES 2k Network is coordinated with the NOAA World Data Center for Paleoclimatology to establish a benchmark database of proxy climate records for the past two millennia (Supplementary Note A).

Reconstruction domains for the PAGES 2k regions reported here encompass 36% of the Earth's surface (Fig. 1). Although the regions largely coincide with the continents rather than climatological criteria, the annual mean temperature averaged over these regions explains 90% of the global mean annual temperature variability in the instrumental record (Supplementary Fig. S1). Suitable proxy records from Africa (Supplementary) are currently too sparse for a reliable temperature synthesis[8], and analysis of paleoceanographic data by the recently formed Ocean 2k group is in progress[9]. Each regional group identified the proxy climate records that best enable reconstruction of annual or warm-season temperature variability within their region, using *a priori* established criteria (Supplementary Database S1). The PAGES 2k dataset includes 511 time series of tree rings, pollen, corals, lake and marine sediment, glacier ice, speleothems, and historical documents that record changes in biological or physical processes sensitive to temperature variations.

Except for North America, the PAGES 2k reconstructions have annual resolution (Supplementary Fig. S2; Database S2). Three of the temperature reconstructions span approximately 2000 years (Arctic, Europe, Antarctica), and three cover the past 1000 to 1200 years (Asia, South America, Australasia). The North American region includes a short annually resolved tree-ring-based reconstruction (to 1200 CE) and a longer 30-year-resolved pollen-based reconstruction (to 480 CE).

Each continental-scale temperature reconstruction was derived using different statistical methods, with each 2k Network group tailoring its procedures to the strengths of their regional proxy records and calibration targets (Supplementary Part II). Most groups used either a scaling approach to adjust the mean and variance of a predictor composite to an instrumental target, or a regression-based technique to extract a common signal from the predictors using principal components or distance weighting (Table 1). Some of the heterogeneities among the regional temperature reconstructions might be due to differences in reconstruction methods, which may underestimate the amplitude of low-frequency variability differently[10]. In addition, differences between regional reconstructions may reflect differences in their reconstruction targets (land only versus land and ocean), proxy types, and proxy-dating uncertainties. Temperature variability also differs between summer and annual reconstructions, although the two are correlated in meteorological records from our regions (average r-value = 0.73 ± 0.08; Table 1). Screening proxy records based on their statistical similarity to a common instrumental target, as was done for most regional reconstructions, can hamper interpretations that involve comparing the variability of temperature during the 20th century to that of earlier periods[11]. To address these issues, and to assess the extent to which the choice of reconstruction method might influence our conclusions, we applied uniform procedures to the same proxy data to generate three additional reconstructions from each region (Supplementary Note B); these are referred to as ‘alternative reconstructions’.

Our analysis of multi-decadal variability focuses on 30-year-mean temperatures (three calendar decades) and their standardized values (Fig. 3; Supplementary Database S2). This temporal resolution enables the inclusion of the 30-year-resolved pollen-based reconstruction from North America. Using standardized values circumvents regional differences in the magnitude of temperature variability, which depends on geographical factors and can be influenced by the seasonal bias of proxy types.

Millennial cooling

Over their respective record lengths, all regions experienced a long-term cooling trend followed by recent warming during the 20th century, except Antarctica. Before 1900 CE (Supplementary Table S2 includes an analysis of regressions up to both 1900 and 1850 CE), the cooling trend is significant ($p < 0.05$) in all regions except North America where the cooling trend is weakly significant ($p < 0.10$) in the tree-ring reconstruction, and not significant in the pollen reconstruction. The regional rate of cooling varies between about 0.1 and 0.3°C per 1000 years. Since 1000 CE — the interval represented in all regions — the trends are also significant, except for Europe ($p = 0.13$). In general, the overall trends in the 30-year-averaged PAGES 2k Network reconstructions agree with those in the alternative reconstructions (Table S2). They are also consistent with the cooling of global sea-surface temperatures from year 1 to1800 CE exhibited in the PAGES Ocean2k synthesis[9].

The individual site-level proxy records were also analyzed to determine the extent to which the long-term cooling trend is a common feature, an approach that is independent of the reconstruction procedures. Generally, the longer the proxy record, the more likely it is to exhibit a significant long-term cooling trend (Fig. 2). For example, of the 24 individual records from all regions that extend back to 1 CE, 20 have negative slopes between year 1 and 1900 CE (Supplementary Fig. S6), which is unlikely to occur by chance (one-tailed sign test, $p < 0.001$). Of these, three-quarters are statistically significant ($p < 0.05$). Of the 90 records that

extend to 1000 CE, 54 have negative slopes (sign test, $p < 0.03$), over one-third of which are statistically significant ($p < 0.05$).

The regression analysis of the cooling trend is supported by temperature differences at multi-centennial scales. The three longest reconstructions (Arctic, Europe and Antarctica) show higher temperatures during the early centuries of the first millennium compared with those of the late (pre-20th) centuries of the second millennium. Commensurate cooling occurred during the last millennium; for example, the first four centuries (1000-1400 CE) were warmer than the following four centuries (1400-1800 CE) in all regions, despite cooling that starts between 1200 and 1300 CE in the Arctic, Europe and Asia. The average temperature difference between the four-century intervals averaged over all the regions was about 0.1°C, which is consistent with the underlying millennial-scale cooling trend (roughly -0.2°C per 1000 years).

Several studies have investigated the cause of cooling between the 10th and 16th centuries, suggesting a potential role of solar irradiance, volcanic activity, land-cover changes and orbital-driven insolation[6,12,13,14,15]. An ensemble of simulations performed with a climate model of intermediate complexity (Supplementary Note C) shows that these four forcings are the dominant cause of the annual mean cooling trend simulated between 900 and 1850 CE, with the relative contribution of each forcing varying among regions (Table S4). The same forcings have likely played a similar role on a longer time-scale including the entire first millennium. For example, some records of volcanic[16] and solar[17] activities (Fig. 4f) show significant long-term negative forcing over the last 2000 years (Mann-Kendall trend test, $p < 0.05$). Furthermore, in the Northern Hemisphere mid to high latitudes, the millennial-scale cooling can be ascribed to a decrease in orbital-driven local summer insolation, as suggested for the Arctic[18] and northern Scandinavia[19]. In the Southern Hemisphere, a climate model of intermediate complexity simulates a multi-millennial cooling in summer as a delayed response

to the decrease in local spring insolation, modulated by the thermal inertia of the Southern Ocean[20].

Multi-decadal to centennial variability

Temperatures did not fluctuate uniformly among all regions, highlighting the regionally specific evolution of temperature at multi-decadal to centennial time scales (Fig. 3). However, the period from around 830 to 1100 CE generally encompassed a sustained warm interval in all four Northern Hemisphere regions. In South America and Australasia, a sustained warm period occurred later, from around 1160 to 1370 CE. In the Arctic and Europe, temperatures were relatively high during the first centuries of the CE. Most other reconstructions are too short and based on too few proxy records to infer temperatures prior to around 1000 CE.

The transition to colder regional climates between 1200 and 1500 CE occurred earlier in the Arctic, Europe and Asia than in North America or the Southern Hemisphere. Differences among regions could reflect non-forced variability involving the major modes of atmospheric variability[21,22]. By around 1580 CE all regions except Antarctica entered a protracted cold period. Apart from intervals of relative regional warmth, especially during the 18th century, cold conditions prevailed until late in the 19th century. Again, the alternative reconstructions show patterns similar to those of the PAGES 2k regional reconstructions (Fig. S4).

Paleoclimate records spanning the last millennium are often characterized as including some manifestation of a warm Medieval Warm Period (MWP) followed by a cool Little Ice Age (LIA)[23]. Previous reviews of these intervals have shown a tendency for centennial-scale temperature anomalies, but have also emphasized their heterogeneity through space and time[6,24,25,26,27.] Our regional temperature reconstructions (Fig. 3) also show little evidence for globally synchronized multi-decadal shifts that would mark well-defined worldwide MWP and LIA intervals. Instead, the specific timing of peak warm and cold intervals varies regionally,

with multi-decadal variability resulting in regionally specific temperature departures from an underlying global cooling trend.

Our regional temperature reconstructions can be compared with records of solar irradiance and volcanic activity to examine the extent to which temperature changes coincide with these climate forcings. The time series of area-weighted, standardized 30-year-mean temperatures averaged across all regions (Fig. 4b) displays broad similarities with records of climate forcings (Fig. 4f,g), a feature also apparent in previously published reconstructions of Northern Hemisphere average temperature (Fig. 4a). The periods of most negative volcanic-solar forcing (nine 30-year periods clustered in five distinct 30- to 90-year intervals between 1251 and 1820, as determined using criteria specified in Methods) generally correspond to a drop in the averaged temperature (Fig. 4b). Monte Carlo sampling of the detrended global time series shows that the averaged temperature during these perturbed intervals was significantly lower ($p < 0.01$) than the means of nine randomly selected 30-year periods between 830 and 1910 CE. At the regional scale, these volcanic-solar-perturbed periods include the coolest 30-year period of each reconstruction, although the response in Australasia and North America seems to lag by one 30-year period during the 19th century, and Antarctica was coldest during the middle of the 20th century (Fig. 3). Not all regions cooled during each of the strong volcanic-solar downturns. For example, Australasia, South America and North America tree rings do not show multi-decadal cooling during the earliest interval of strong negative forcing (1251-1310 CE).

20th century reconstructed temperature

The 20th century ranked as the warmest or nearly the warmest century in all regions except Antarctica where the large thermal inertia of the surrounding ocean may dampen warming[28]. Excluding Antarctica, the 20th-century average temperature among the six regions was about 0.4 higher than the averaged temperatures of the preceding five centuries (Supplementary

Table S3 lists centennial temperature differences based on alternative reconstructions).

Compared to the preceding five centuries, 20th-century warming in the four northern hemisphere regions was on average about twice that of the more strongly ocean-dominated regions of Australasia and South America (about 0.5°C compared with 0.2°C), with the greatest differences at northern high latitudes. Twentieth-century warming in the Arctic (0.9°C) was about three times that of the average of the other five non-polar regions.

Our best estimate of reconstructed temperature for 1971-2000 CE can be compared with all other consecutive 30-year periods within each regional reconstruction. In Asia and Australasia, reconstructed temperature was higher during 1971-2000 than any other 30-year period. The Arctic was also warmest during the 20th century, although likely warmer during 1941-1970 than 1971-2000 according to our reconstruction. In South America, the 1971-2000 reconstructed temperature was similar to the record maximum in 1251-1280 CE. In North America, the reconstructed temperature for the 1971-2000 bin does not include the warm decades since 1980, and therefore underestimates the actual temperature for that interval. In Europe, slightly higher reconstructed temperatures were registered in 740-770 CE, and the interval from 21-80 CE was substantially warmer than 1971-2000. Antarctica was likely warmer than 1971-2000 as recently as 1671-1700 CE, and the entire period from 140-1250 was warmer than 1971-2000. These interpretations are generally supported by the relative magnitude of recent warming in the alternative reconstructions (Supplementary Fig. S4; Database S2).

Each individual proxy record contributing to the regional reconstructions was analyzed to evaluate whether the values during 1971-2000 indicate higher temperatures than for any other 30-year period (Fig. 4d,e), independent of the procedures used for calibrating the temperature reconstructions. According to this analysis, of the 323 individual proxy records that extend to 1500 CE, more sites appear warmest during 1971-2000 than during any other 30-year period, both in terms of the total number and their proportion in each region. Similarly, of the 52

individual records that extend to 500 CE, more sites (and a higher proportion) appear warmest during the 20th century than during any other century. Albeit, the fraction of individual records that indicates the highest temperatures during 1971-2000 decreases with increasing record length.

The area-weighted average of the best estimate of past temperature from all seven regions indicates that 1971-2000 was warmer than anytime in nearly 1400 years (Fig. 4b), keeping in mind that this analysis does not consider the uncertainty associated with the temperature estimates, and that the reconstructions are different lengths. Area-weighted averages of the three alternative reconstructions agree with this assessment (Supplementary Fig. S5). Large uncertainties remain, especially during the first millennium when only some regions are represented. Regardless, the global warming that has occurred since the end of the 19th century reversed a persistent long-term global cooling trend. The increase in average temperature between the 19th and 20th centuries exceeded the temperature difference between all other consecutive centuries in each region, except Antarctica and South America.

The PAGES 2k Network reconstructions show clear regional expressions of temperature variability at the multi-decadal to century scale, whereas a long-term cooling trend prior to the 20th century is evident globally. Centennial-scale temperature changes in Australasia and South America generally follow those of the Northern Hemisphere regions, while temperature changes in Antarctica do not correlate with those of other regions. The pre-20th-century long-term global cooling trend is evident in differences in average temperature between multi-centennial periods, and in the significance of the slopes of least-squares linear regressions for both the regional reconstructions and the individual site-level proxy records. Our reconstructions and proxy-data compilation will be useful in future studies, including as a benchmark for comparisons with climate-model simulations aimed at understanding the cause

of the global cooling, and the extent to which externally forced and unforced variability can explain temperature fluctuations and trends at the continental scale.

Methods

Data sources. All proxy records used for the regional reconstructions are included in Supplementary Database S1, and are archived by the NOAA World Data Center for Paleoclimatology (www.ncdc.noaa.gov/paleo/pages2k/pages-2k-network.html). All regional temperature reconstructions are included in Database S2.

Relation between proxy records and temperature. The sign (i.e., positive or negative) of the correlation between each proxy record and temperature is listed in Database S1. These were determined using different approaches for different regions. In the Arctic, the relation is adopted from the publication of the original records. In Europe, the 11 inputs to the regional reconstruction include 10 tree-ring composites and documentary evidence, all calibrated to temperature. The North America pollen-based reconstruction also relies on regional syntheses that were previously transformed into temperature. For Asia and Antarctica, only records with demonstrated positive correlations with local or regional (respectively) instrumental data were included in the reconstructions. The North America tree-ring, South America and Australasia reconstructions were based on principal component regression methods, therefore any proxy record can contribute with either a positive or negative temperature relation with different principal components, or for ensemble members with different instrumental targets. Furthermore, in spatially explicit reconstructions (North America tree rings, Australasia and South America), the sign of the contribution for each record can vary spatially as well. Therefore, we determined the temperature sign relation for these three regional reconstructions based on the direction of the correlation between the proxy records and the area-weighted average mean annual temperature from the domain areas in Figure 1 using the HadCRUT4 (ref.[29]) data series.

Significance of trends. The significance of long-term cooling trends in the reconstructions (Table S2) and in the individual site-level proxy records (Figs. 2, S6) was calculated at the p = 0.05 confidence level using a 1-sided Student's t-test, while accounting for lag-1 autocorrelation in both the calculation of standard error and in indexing the t-values[30]. Trends in the individual proxy records (site level) were determined by first inverting those proxy records having a negative correlation with temperature (as described above). The pre-1900 trend in each record was analyzed for successively shorter segments of time, beginning with the entire time series, then truncating each series by 30-year intervals, with each segment ending in 1900 CE. The trend in each truncated series was determined by the slope of its linear regression. For illustration purposes, the fraction of positive trends with magnitude larger than the 1-sided p = 0.05 level are shown in Figure 2.

Volcanic-solar downturns (Figs. 3 & 4). We analyzed two time series of solar forcing and two of volcanic forcing from ref. [31] (Fig. 4g), the volcanic series from ref.[16] (Fig. 4f), and the solar series from ref.[17] (Fig. 4f) to discern periods of strongest agreement and magnitude of forcing. Each time series was binned into 30-year intervals that coincide with the temperature reconstructions (bin centers from 845 to 1985 CE). The eight bins (21% of each record) with most negative forcing were selected from each series; then, the subset of bins overlapping among at least one-half (≥3) of the six time series was identified. The nine 30-year bins defined this way comprise the five intervals that we term "volcanic-solar downturns": 1251-1310, 1431-1520, 1581-1610, 1641-1700 and 1791-1820 CE.

Temperatures during volcanic-solar downturns. To evaluate whether temperatures were significantly lower during intervals of negative climate forcing, we implemented a Monte Carlo procedure to randomly sample the area-weighted regional temperatures between 830 and 1910 CE (we excluded the warm 20th century (1910-2000 CE) to make the test more conservative). For each of 10,000 iterations, the mean temperature of nine 30-year intervals was calculated. Because most of the intervals of negative forcing occur later in the record, the

low temperatures during these intervals may be partially due to long-term cooling. To assess this possibility, we also conducted the test on the detrended area-weighted mean. For both the original and detrended tests, the mean of the nine intervals of negative solar and volcanic forcing was lower than more than 99% of the means of randomly selected intervals (i.e., $p < 0.01$).

Warmest intervals within individual proxy records (Fig. 4d,e). Site-level warmest-interval analysis was conducted for 30-year intervals spanning from 1490 to 2000 CE, and for 100-year intervals between 500 and 2000 CE. Proxy records with negative correlation with temperature were inverted. Only records with at least one measurement in each 30- or 100-year bin were used. The three tree-ring records from northern Fennoscandia, which were used in both the Arctic and the Europe reconstructions, were included only once in the site-level analysis. The warmest intervals were identified by ranking the values of the 30- or 100-year bins for each record. To better represent regions with fewer records, the values were presented as the fraction of records in each region, rather than the number of records. The fractions were scaled such that a value of 1 corresponds to all records in all regions.

Address correspondence and requests for materials to: darrell.kaufman@nau.edu

Acknowledgments

Support for PAGES activities is provided by the US and Swiss National Science Foundations and by the US National Oceanographic and Atmospheric Administration. All maps were kindly created by Alexander Hermann, Institute of Geography, University of Bern.

Author Contributions

Writing team: D.S.K. led the synthesis; N.P.McK., E.Z. & S.T.H. performed the synthesis analyses; D.S.K., R.N., L.v.G., T.K., H.G., H.W., C.S.M.T., F.C.L., V.M-D., E.R.W., & T.v.O. prepared the manuscript. **Africa**: D.J.N., A.A., B.M.C., S.W.G., S.E.N., T.M.S, D.V., A-M.L.,

M.U. compiled and evaluated the proxy data. **Antarctica**: T.v.O, M.B., A.D.M., R.M., H.O., M.Se., B.S., E.J.S., M.T., J.W.C.W., M.A.J.C., J.R.McC., M.Si. & B.M.V. provided proxy data, contributed to their dating and interpretation; M.A.J.C., J.R.McC., M.Si. & B.M.V. correlated volcanic markers; T.v.O & R.N. produced the reconstruction; M.A.J.C. managed the data. **Arctic**: A.A.K., D.S.K. & S.T.H. coordinated the study. S.T.H, D.S.K. & F.C.L. collected and reviewed the proxy data; S.T.H. calculated the reconstruction and managed data. **Asia**: M.A., K.J.A., H.P.B., B.M.B.,Q.G., E.R.C., Z.F., N.P.G., K.K., P.J.K., T.N., J.G.P., M.Sa., X.S., O.N.S. & K.Y. contributed, collected and analyzed the proxy data; K.J.A., B.M.B., E.R.C. & P.J.K. performed the reconstruction; T.N., M.Sa. & F.S. provided technical support and managed the data. **Australasia**: J.G., A.M.L., S.J.P. & R.N. coordinated the study. R.N. & J.G. collated, managed and analyzed the proxy data; R.N. & J.G. developed the reconstruction with input from S.J.P. **Europe**: U.B., J.E., S.W., E.Z., D.McC., F.J.G.-R., F.C.L., J.E.S., J.P.W. & J.L. collected, reviewed and analyzed the proxy records, and provided input in the analysis and interpretation of the European reconstruction; S.W. managed the data; J.P.W. & J.E.S. produced the reconstruction. **North America**: H.F.D., E.R.W., V.T., R.G., N.G. & A.E.V. designed the study, analyzed the data, and produced the reconstructions; E.R.W. & A.E.V. collected and archived the data. **South America**: R.V. & M.G. coordinated the study; R.V., D.A.C, A.L., I.A.M., M.S.M., L.v.G., M.R.P. & A.R. provided proxy data; R.N. calculated the reconstruction; R.N. & I.A.M. managed the data. All authors reviewed the manuscript.

Additional information

The authors declare no competing financial interests. Supplementary information accompanies this paper on www.nature.com/naturegeoscience. Reprints and permissions information is available online at http://npg.nature.com/reprintsandpermissions. Correspondence and requests for materials should be addressed to D.S.K.

Table references

32 33 34 35 36 37 38 39 40 41 42

Figure Captions

Figure 1 | The PAGES 2k Network. Boxes delimit the continental-scale regions used in this study. The pie charts represent the fraction of proxy data types used for each regional reconstruction. Supplementary Database S1 includes information about each study site and the proxy data for all time series used in the regional reconstructions.

Figure 2 | Summary of long-term trends within individual site-level proxy records. Sign and statistical significance of the slope of least-squares linear regression through each site-level proxy record within the PAGES 2k dataset. The fraction of records that exhibit significant ($p < 0.05$) or non-significant cooling trends was evaluated for records extending back different lengths in 30-year steps. The longer the record, the more likely it is to exhibit a significant long-term cooling trend. For illustration purposes, the fraction of positive trends with magnitude smaller (light red) and larger (red) than the 1-sided $p = 0.05$ level is also included.

Figure 3 | Continental-scale temperature reconstructions. Thirty-year mean temperatures for the seven PAGES 2k Network regions, standardized to have the same mean (zero) and standard deviation (one) over the period of overlap among records (1190-1970 CE). North America includes a shorter tree-ring-based and a longer pollen-based reconstruction. Dashed-rounded rectangles enclose intervals of pronounced volcanic and solar negative forcing since 850 CE (see Methods). Lower panel shows running count of number of individual proxy records by region. Data are listed in Database S2.

Figure 4 | Composite temperature reconstructions with climate forcings and previous hemisphere-scale reconstructions. **a,** Previously published Northern Hemisphere 30-year-mean temperature reconstructions relative to the 1960-1991 reference period (ref.[5,43,44,45]). **b,** Standardized 30-year-mean temperatures averaged across all seven continental-scale

regions. Blue symbols are area-weighted averages using domain areas listed in Table 1, and bars show 25th and 75th percentiles to illustrate the variability among regions; open black boxes are medians. Red line is the 30-year-average annual global temperature from the HadCRUT4 (ref.[29]) instrumental time series relative to 1960-1991, and scaled visually to match both the standardized values over the instrumental period and the temperature scale in panel (**a**). **c,** Running count of the number of regional reconstructions. **d,** For each 30-year period since 1500 CE, proportion of individual proxy records within each region that indicate the highest temperature during that 30-year period. **e,** For each century since 500 CE, proportion of individual proxy records within each region that indicate the highest temperature during that century. **f,** Long-term volcanic forcing from ref.[16] (black curve; spikes beyond -8 Wm^{-2} are truncated), and solar forcing from ref.[17] (red curve). **g**, Radiative forcings relative to 2000 CE smoothed using 30-year averages from ref.[31], including: (i) two estimates of volcanic forcing[46,47]; (ii) two estimates of solar forcing that span the range from strong[48] to weak[49]; and (iii) well-mixed greenhouse gases relative to 850 CE. **h,** Change in summer (Jul/Jan) insolation at 65°N/S and 15°N/S latitudes relative to 2000 CE from ref.[50]. Vertical red bands indicate volcanic-solar downturns as defined in Methods.

Table 1 | Summary of continental-scale proxy temperature reconstructions used in this study.

Region & (area 10^6 km^2)	Time period (CE)	Proxy type & (N°)	Reconstruction target	Ann-sum r value[a]	Reconstruc-tion method[b]	Calibration r value[c]	Major references (N°)
Arctic (34.4)	1-2000	Lake sediments (22) Ice cores (16) Tree rings (13) Marine sediments (6) Documentary (1) Speleothem (1)	Mean annual Land & ocean	0.79	PaiCo	0.56	Hanhijärvi (32) Kaufman (18)
Europe (13.0)	1-2003	Tree rings (10) Documentary (1)	Summer (JJA) Land only	0.66	CPS	0.85	Büntgen (33) Esper (19) Dobrovolný (34)
Asia (31.1)	800-1989	Tree rings (229)	Summer (JJA) Land only	0.71	PPR	0.52	Cook (35)
North America (12.5)	1204-1974 480-1950	Tree rings (146) Pollen (4 ecoregions)	Mean annual Land & ocean	0.68	PCSR PCA	0.96 0.56[d]	Wahl (36) Viau (37)
South America (20.0)	857-1995	Tree rings (15) Instrumentals (4) Ice cores (2) Marine sediment (1) Lake sediment (1)	Summer (DJF) Land only	0.82	PCR/CPS	0.82	Neukom (38)
Australasia (37.9)	1001-2001	Coral (12) Tree rings (14) Speleothem (1)	Warm season (SONDJF) Land & ocean	0.80	PCR	0.80	Gergis (39)
Antarctica (34.4)	167-2005	Ice cores (11)	Mean annual Land only	0.62	CPS	0.60	Schneider (40) Steig (41)

[a] Correlation between annual and summer (JJA or DFJ) temperatures based on HadCRUT4, 1850-2012 and using land or land & ocean as per the reconstruction targets; correlation for Australasia is for the warm season (SONDJF).

[b] See Supplementary Information; PaiCo = pairwise comparison; PCA = principal component analysis; PCR = Principal component reconstruction; PCSR = principal components spatial regression; CPS = composite plus scaling; PPR = point-by-point regression.

[c] r and p values were calculated for the correlation between reconstructed values and target instrumental data using the seasons, calibration period, domains, and gridded instrumental products specified for each region in the Supplemental Information. p-values for calibrations are all < 0.001 as estimated by phase-randomization Monte-Carlo methods that capture the serial correlation structure of the time series (ref. 42).

[d] Square-root of the explained variance (R^2) of the fit of decadal tree-ring-based reconstruction to regional pollen-based reconstructions (0.334) times R^2 of the decadal tree-ring-based calibration itself (0.929); p-value not determined.

References

[1] Rockström, J. *et al*. A safe operating space for humanity. *Nature* **461**, 472-475 (2009).

[2] Snyder, C. W. The value of paleoclimate research in our changing climate. *Clim. Change* **100**, 407-418 (2010).

[3] Braconnot, P. *et al*. Evaluation of climate models using palaeoclimatic data. *Nature Clim. Change* **2**, 417-424 (2012).

[4] Deser, C., Phillips, A., Bourdette, V. & Teng, H. Uncertainty in climate change projections: the role of internal variability. *Clim. Dyn.* **38**, 527 (2012).

[5] Mann, M. E. *et al*. Proxy-based reconstructions of hemispheric and global surface temperature variations over the past two millennia. *Proc. Natl. Acad. Sci. U.S.A.* **105**, 13252-13257 (2008).

[6] Mann, M. E. *et al*. Global signatures and dynamical origins of the Little Ice Age and Medieval Climate Anomaly. *Science* **326**, 1256-1260 (2009).

[7] Frank, D., Esper, J., Zorita, E. & Wilson, R. A noodle, hockey stick, and spaghetti plate: a perspective on high-resolution paleoclimatology. *WIREs Clim. Change* **1**, 507-516 (2010).

[8] Nicholson, S. E. *et al*. Temperature variability over Africa during the last 2000 years. *The Holocene* (in press).

[9] PAGES/Ocean2k Working Group. Synthesis of marine sediment-derived SST records for the past 2 millennia: First-order results from the PAGES/Ocean2k project. Abstract PP11F-07 presented at the 2012 Fall Meeting AGU, San Francisco, CA, 3-7 Dec (2012).

[10] Christiansen, B., Schmith, T. & Thejll, P. A surrogate ensemble study of climate reconstruction methods: Stochasticity and robustness. *J. Clim*. **22**, 951-976 (2009).

[11] Esper, J. & Frank, D. C. Divergence pitfalls in tree-ring research. *Clim. Change* **94**, 261-266 (2009).

[12] Jones, P. D. & Mann, M. E. Climate over past millennia. *Rev. Geophys.* **42**, RG2002 (2004).

[13] Crowley T. J. Causes of climate change over the past 1000 years. *Science* **289**, 270-277 (2000).

[14] Bauer, E., Claussen, M., Brovkin, V. & Huenerbein, A. Assessing climate forcings of the Earth system for the past millennium. *Geophys. Res. Lett.* **30**, (2003), doi:10.1029/2002GL016639.

[15] Hegerl, G. C. *et al*. in *Climate Change 2007: The Physical Science Basis,* S. Solomon *et al.*, Eds. (Cambridge Univ. Press, Cambridge and New York, 2007).

[16] Crowley, T. J., Baum, S. K, Kim, K. –Y., Hegerl, G. C. & Hyde, W. T. Modeling ocean heat content changes during the last millennium, *Geophys. Res. Lett.* **30**, 1932-1935 (2003).

[17] Steinhilber F*. et al.* 9,400 years of cosmic radiation and solar activity from ice cores and tree rings. *Proc. Nat. Acad. Sci.* **109** 5967-5971 (2012).

[18] Kaufman, D. S. *et al.* Recent warming reverses long-term Arctic cooling. *Science* **325**, 1236-1239 (2009).

[19] Esper J. *et al.* Orbital forcing of tree-ring data. *Nature Clim. Change* **2**, 862-866 (2012).

[20] Renssen, H. Goosse, H., Fichefet, T., Masson-Delmotte, V. & Koç, N. The Holocene climate evolution in the high-latitude Southern Hemisphere simulated by a coupled atmosphere-sea ice-ocean-vegetation model. *The Holocene* **15**, 951-964 (2005).

[21] Fernández-Donado, L. *et al.* Large-scale temperature response to external forcing in simulations and reconstructions of the last millennium. *Clim. Past.* **9**, 393-421 (2013).

[22] Goosse, H. *et al.* The role of forcing and internal dynamics in explaining the "Medieval Climate Anomaly". *Clim. Dyn.* **39**, 2847-2866 (2012).

[23] Lamb, H. H. The early medieval warm epoch and its sequel. *Palaeogeogr. Palaeocl.* **1**, 13-37 (1965).

[24] Bradley, R. S., Hughes, M. K. & Diaz, H. F. Climate in Medieval time. *Science* **302**, 404-405 (2003).

[25] Matthews, J. A. & Briffa, K. R. The 'Little Ice Age': Re-evaluation of an evolving concept. *Geogr. Ann.* **87A**, 17-36 (2005).

[26] Ljungqvist, F. C., Krusic, P. J., Brattström, G. & Sundqvist, H. S. Northern Hemisphere temperature patterns in the last 12 centuries. *Clim. Past* **8**, 227-249 (2012).

[27] Diaz, H.F. *et al.* Spatial and temporal characteristics of climate in Medieval times revisited. *B. Am. Meteorol. Soc.* **92/11**, 1487-1500 (2011).

[28] Stouffer R. J., Manabe, S. & Bryan, K. Interhemispheric asymmetry in climate response to a gradual increase of atmospheric CO_2. *Nature* **342**, 660-662 (1989).

[29] Jones, P. D., Lister, D. H., Osborn, T. J., Harpham, C., Salmon, M. & Morice, C. P. Hemispheric and large-scale land surface air temperature variations: An extensive revision and an update to 2010. *J. Geophys. Res.* **117**, D05127 (2012).

[30] Santer, B. D. *et al.* Statistical significance of trends and trend differences in layer-average atmospheric temperature time series. *J Geophy. Res.* **105**, 7337-7356 (2000).

[31] Schmidt, G. A. *et al.* Climate forcing reconstructions for use in PMIP simulation of the last millennium (v1.1). *Geosci. Model Dev.* **5**, 185-191 (2012).

[32] Hanhijärvi, S., Tingley, M. P. & Korhola, A. Pairwise comparisons to reconstruct mean temperature in the Arctic Atlantic region over the last 2000 years. *Clim. Dyn.* (in press).

[33] Büntgen, U. *et al.* 2500 years of European climate variability and human susceptibility. *Science* **331**, 578-582 (2011).

[34] Dobrovolný, P. *et al.* Monthly, seasonal and annual temperature reconstructions for central Europe derived from documentary evidence and instrumental records since AD 1500. *Clim. Change* **101**, 69-107 (2010).

[35] Cook, E. *et al.* Tree-ring reconstructed summer temperature anomalies for temperate East Asia since 800 C.E. *Clim. Dyn.* (in press).

[36] Wahl, E. R. & Smerdon J. E. Comparative performance of paleoclimate field and index reconstructions derived from climate proxies and noise-only predictors. *Geophys. Res. Lett.* **39**, L06703 (2012).

[37] Viau, A. E., Ladd, M., Gajewski, K. The climate of North America during the past 2000 years reconstructed from pollen data. *Glob. Planet. Change* **84-85**, 75-83 (2012).

[38] Neukom, R. *et al.* Multiproxy summer and winter surface air temperature field reconstructions for southern South America covering the past centuries. *Clim. Dyn.* **37**, 35-51 (2011).

[39] Gergis, J. *et al.* Evidence of unusual late 20th century warming from an Australasian temperature reconstruction spanning the last millennium. *J. Clim.* (in revision).

[40] Schneider, D. *et al.* Antarctic temperatures over the past two centuries from ice cores. *Geophys. Res. Lett.* **33**, L16707 (2006).

[41] Steig, E. *et al.* Significance of exceptional recent climate and glacier changes in West Antarctica. *Nat. Geosci.* (in press).

[42] Ebisuzaki, W. A method to estimate the statistical significance of a correlation when the data are serially correlated. *J. Climate* **10**, 2147-2153 (1997).

[43] Moberg, A., Sonechkin, D. M., Holmgren, K., Datsenk, N. M. & Karlén, W. Highly variable Northern Hemisphere temperatures reconstructed from low- and high-resolution proxy data. *Nature* **433**, 613-617 (2005).

[44] Ljungqvist, F.C. A new reconstruction of temperature variability in the extra-tropical Northern Hemisphere during the last two millennia. *Geogr. Ann.* **92**, 339-351 (2010).

[45] Hegerl, G. C., Crowley, T. J., Hyde, W. T. & Frame, D. J. Climate sensitivity constrained by temperature reconstructions over the past seven centuries. *Nature* **440**, 1029-1032 (2006).

[46] Gao, C., Robock, A. & Ammann, C. Volcanic forcing of climate over the past 1500 years: An improved ice core-based index for climate models. *J. Geophys. Res.-Atmosph.* **113**, D23111 (2008).

[47] Crowley, T. & Unterman, M. Technical details concerning development of a 1200-year proxy index for global volcanism. *Clim. Past Discus.* doi:10.5194/essdd-5-1-2012.

[48] Shapiro, A. *et al*. A new approach to the long-term reconstruction of the solar irradiance leads to large historical solar forcing. *Astron. Astrophys.* **529**, A67 (2011).

[49] Vieira, L. E., Solanki , S. K., Krivov, A. V. & Usoskin, I. G. Evolution of the solar irradiance during the Holocene. *Astron. Astrophys.* **531**, A6 (2011).

[50] Berger, A. L. Long-term variation of daily insolation and Quaternary climatic change. *Quat. Res.* **9**, 139-167 (1978).

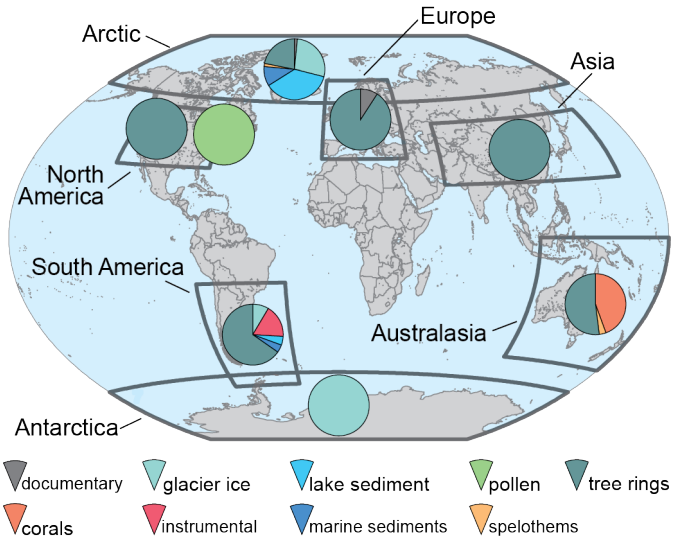

PAGES 2k Consortium
Figure 1

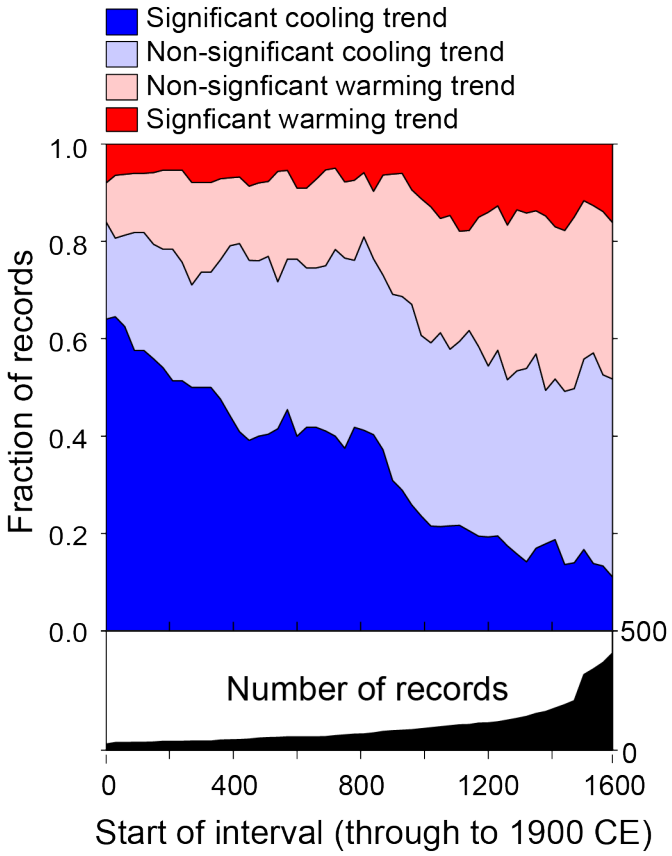

PAGES 2k Consortium
Figure 2

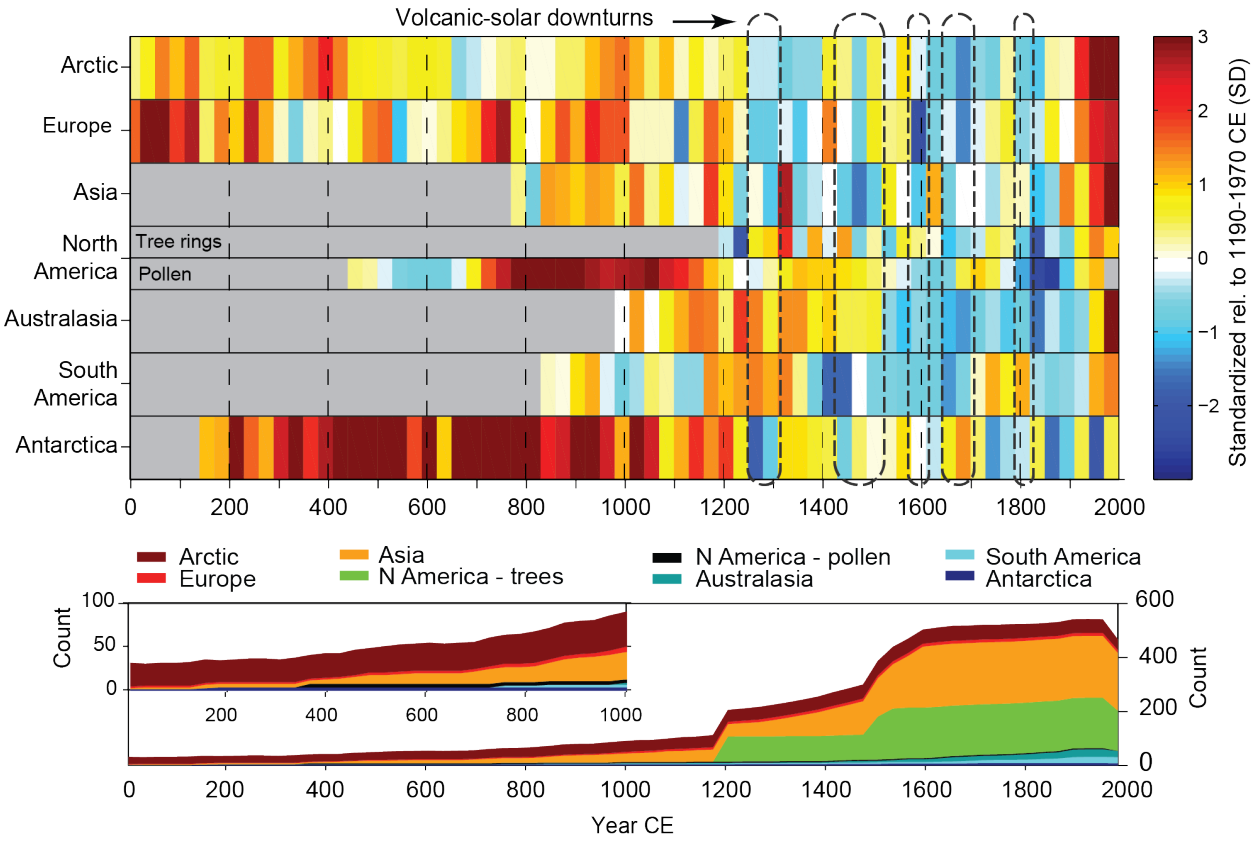

PAGES 2k Consortium
Figure 3

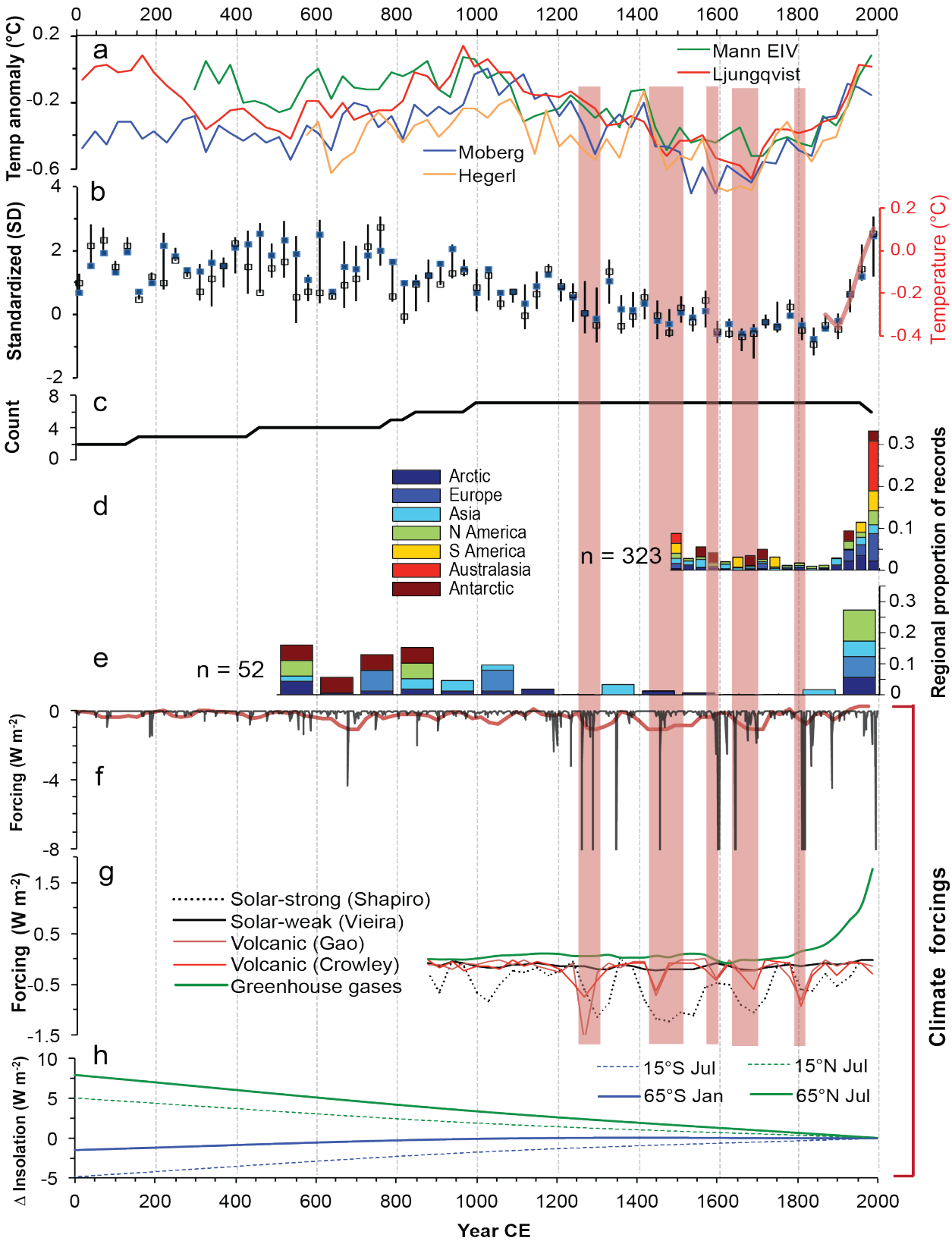

PAGES 2k Consortium – Figure 4